

# The general cancellation of ladder graphs at finite temperature

M. E. Carrington <sup>a</sup> and R. Kobes <sup>b</sup>

<sup>a</sup> *Department of Physics*

*Winnipeg Institute of Theoretical Physics*

*University of Brandon*

*Brandon, Manitoba, R7A 6A9*

*Canada*

<sup>b</sup> *Department of Physics*

*Winnipeg Institute of Theoretical Physics*

*University of Winnipeg*

*Winnipeg, Manitoba, R3B 2E9*

*Canada*

(September 1, 2018)

## Abstract

In some cases, an important example being at finite temperature, extreme infrared, collinear, or light-cone behaviour may cause the usual loop expansion to break down. For some of these cases higher order ladder graphs can become important. In an earlier paper it was shown that, given a particular relation between a vertex and a self-energy function, the resummation of the ladder graphs simplifies significantly when other types of graphs are included in a consistent effective expansion. In this paper we show that this assumed relation is valid for a large class of vertex and self-energy functions at finite temperature.

PACS numbers: 11.10Wx, 11.15Tk, 11.55Fv

## I. INTRODUCTION

Particularly at finite temperature, infrared divergences can cause the loop expansion to fail. In many cases this problem can be resolved by using an effective expansion based on the hard thermal loops [1–6]. This expansion does not solve all such problems, however; we mention in this context the damping rate of a fast fermion, where a self-consistent calculational scheme outside of the hard thermal loop expansion has been used [7,8], processes sensitive to the behaviour near the light-cone, where an “improved” hard thermal loop expansion has been proposed [9,10], the calculation of the pressure [11], and the problem of the effective potential in electro-weak theory [12].

In this paper we consider perturbation expansions beyond the loop expansion which include ladder graphs. These graphs, which are not included in the hard thermal loop expansion, become important in certain cases sensitive to the infrared and/or light-cone limits [7,10,11,13], and also arise in the context of the eikonal expansion of gauge theories [14,15]. We show for the calculation of a self-energy that there is an effective expansion for these graphs which arises as the iterative solution of a type of Schwinger–Dyson equation. However, in general other types of graphs must be included in a consistent effective expansion. In this regard, when a relation of the generic form

$$\Gamma(K, P) \approx -ig \frac{1}{K^2 + 2K \cdot P} [\Pi(P) - \Pi(K + P)] \quad (1)$$

between the vertex function  $\Gamma(K, P)$  and a self-energy function  $\Pi(P)$  holds, the inclusion of the non-ladder graphs gives rise to a significant simplification in the expression for the self-energy [28]. We show here that this relation is valid for a large class of vertex and self-energy functions at finite temperature. Finally, if certain assumptions are made on the relative size of the self-energy function  $\Pi(P)$ , we show that the ladder graphs actually cancel against other types of terms.

## II. LADDER GRAPHS

We begin by showing under what circumstances ladder graphs are important. We work here with a scalar  $\phi^3$  theory at zero temperature, but the results generalize straightforwardly for other theories and to finite temperature. Consider first the graph of Fig.1, which is given by

$$-i\Pi(K) = (-ig)^6 \int dR_1 dR_2 dP D(P + R_1 + R_2) D(P + R_1 + R_2 + K) D(R_1) D(P + R_2) \\ D(P + R_2 + K) D(R_2) D(P) D(P + K), \quad (2)$$

where  $D(K) = 1/(K^2 + i\epsilon)$  and  $K = (k_0, \vec{k})$ . In cases where the loop expansion is valid this graph would be suppressed by a factor of  $g^4$  relative to the one-loop graph of Fig. 2. However, especially at finite temperature, circumstances may arise where this is not the case. Let us split two of the propagators in Eq. [2] as

$$D(P + R_2) D(P + R_2 + K) = \frac{D(P + R_2) - D(P + R_2 + K)}{K^2 + 2K \cdot (P + R_2)}, \quad (3)$$

and furthermore consider the infrared limit  $2K \cdot R_2 \ll (K^2 + 2K \cdot P)$ , whereby this splitting is approximated by

$$D(P + R_2)D(P + R_2 + K) \approx \frac{D(P + R_2) - D(P + R_2 + K)}{K^2 + 2K \cdot P}, \quad (4)$$

We perform an analogous split for  $D(P + R_1 + R_2)D(P + R_1 + R_2 + K)$ . Such approximations in Eq. [2] lead to

$$\begin{aligned} -i\Pi(K) \approx & (-ig)^6 \int dR_1 dR_2 dP \frac{D(P + R_1 + R_2) - D(P + R_1 + R_2 + K)}{K^2 + 2K \cdot P} D(R_1) \\ & \frac{D(P + R_2) - D(P + R_2 + K)}{K^2 + 2K \cdot P} D(R_2) D(P) D(P + K). \end{aligned} \quad (5)$$

Now, if it happens that a region of phase space exists where  $(K^2 + 2K \cdot P)$  is sufficiently small (for example, at finite temperature when  $(K^2 + 2K \cdot P) \sim O(g^2 T^2)$ ), then a factor of  $g^4$  arises in the denominator of Eq. [5] which would cancel a factor of  $g^4$  in the numerator. This would lead to a situation where the ladder graph of Fig. 1 is of the same order as the one-loop term of Fig. 2, signaling the breakdown of the loop expansion.

The breakdown of the loop expansion in this manner is due to the importance of the ladder graph in Fig. 1 and similar higher loop ladder graphs. Higher loop “crossed ladders” such as that illustrated in Fig. 3, and given by

$$\begin{aligned} -i\Pi(K) = & (-ig)^6 \int dR_1 dR_2 dP D(P + R_1 + R_2) D(P + R_1 + R_2 + K) D(R_1) D(P + R_2) \\ & D(P + R_1 + K) D(R_2) D(P) D(P + K), \end{aligned} \quad (6)$$

do not contribute in the same way as the ladder graphs. This can be seen as follows. The product of propagators  $D(P + R_1 + R_2)D(P + R_1 + R_2 + K)$  can be split along the lines of Eq. [4], the product  $D(P + R_2)D(P + R_1 + K)$  would be split as

$$D(P + R_2)D(P + R_1 + K) = \frac{D(P + R_2) - D(P + R_1 + K)}{K^2 + 2K \cdot (P + R_1) + (P + R_1)^2 - (P + R_2)^2}. \quad (7)$$

The infrared limit  $2K \cdot R_1 \ll (K^2 + 2K \cdot P)$  then would produce

$$D(P + R_2)D(P + R_1 + K) \approx \frac{D(P + R_2) - D(P + R_1 + K)}{K^2 + 2K \cdot P + (P + R_1)^2 - (P + R_2)^2}, \quad (8)$$

which, in the region  $(K^2 + 2K \cdot P) \sim O(g^2 T^2)$ , would not by itself lead to a cancellation of a factor of  $g^2$  in the numerator due to the presence of the  $(P + R_1)^2 - (P + R_2)^2$  term. One could try to get such a cancellation by furthermore restricting the phase space so that  $P \cdot R_i$  and  $R_i^2$  ( $i = 1, 2$ ) are sufficiently small, but this introduces extra factors of  $g$  in the numerator coming from the momentum integral over  $P$ . The conclusion one draws is that in this infrared limit such crossed graphs are suppressed relative to the ladder graphs.

### III. LADDER RESUMMATION

In this section we describe a method for including the ladder graphs discussed in the previous section in an effective expansion. To this end, we first consider the one-loop vertex of Fig. 4. The expression for this graph is

$$\Gamma(K, P) = (-ig)^3 \int dR D(R) D(R+P) D(K+P+R). \quad (9)$$

We split the two propagators  $D(R+P)D(K+P+R)$  as in Eq. [4] and use the approximation  $2K \cdot R \ll (K^2 + 2K \cdot P)$ . Comparing the result of this operation,

$$\Gamma(K, P) \approx (-ig)^3 \frac{1}{K^2 + 2K \cdot P} \int dR D(R) [D(R+P) - D(K+P+R)], \quad (10)$$

to the one-loop self-energy graph of Fig. 2,

$$-i\Pi(P) = -(-ig)^2 \int dR D(R) D(R+P), \quad (11)$$

we find the relation

$$\Gamma(K, P) \approx -ig \frac{1}{K^2 + 2K \cdot P} [\Pi(P) - \Pi(K+P)]. \quad (12)$$

Note that, due to the absence of an  $i\epsilon$  in the denominator, we must assume in this expression that we are in a region of phase space where  $K^2 + 2K \cdot P$  does not vanish.

Similar results as in Eq. [12] hold in gauge theories. For example, in fermionic  $QED$ , the analogous result is [13]

$$\Gamma_\mu(K, P) \approx -ig \frac{K_\mu + 2P_\mu}{K^2 + 2K \cdot P} [\Pi(P) - \Pi(K+P)], \quad (13)$$

where the one-loop self-energy graph is shown in Fig. 2 (with the photon line having momentum  $R$ ). This relation illustrates the connection between this approximation for the vertex function and gauge invariance: contracting Eq. [13] with  $K^\mu$  leads to

$$K \cdot \Gamma(K, P) = -ig [\Pi(P) - \Pi(K+P)], \quad (14)$$

which of course is the Ward identity for the vertex function. In a sense, this approximation for the vertex function is equivalent to “solving” the Ward identity for this function in the infrared limit.

These considerations allow us to construct a method for generating the ladder graphs. To this end, consider the equation indicated in Fig. 5 for the full self-energy: note that, due to the use of the bare rather than full propagators on the internal lines, this is a “partial” Schwinger–Dyson equation. In momentum space this equation is

$$-i\Pi(K) = ig \int dR \Gamma(K, R) D(R) D(K+R), \quad (15)$$

where  $\Gamma(K, R)$  is the full three-point vertex. Use of Eq. (12) for the full vertex function in terms of the self-energy  $\Pi$  then generates a perturbative summation of ladder graphs,

such as in Fig. 1, under the appropriate approximations of small loop momenta used in the derivation. To illustrate this point, if for the first iteration we use  $\Gamma(K, R)$  of Eq. (12) with the one-loop self-energy of Fig. 2 given in Eq. (11), we find

$$\begin{aligned}
-i\Pi(K) &= (-ig)^2 \int dR \frac{[\Pi(R) - \Pi(K+R)]}{K^2 + 2K \cdot R} D(R)D(K+R) \\
&= (-ig)^2 \int dR \frac{D(R)D(K+R)}{K^2 + 2K \cdot R} i(-ig)^2 \int dR' \\
&\quad [D(R')D(R+R') - D(R')D(K+R+R')] \\
&= i(-ig)^4 \int dR dR' D(R)D(K+R)D(R')D(R+R')D(K+R+R'), \quad (16)
\end{aligned}$$

where we assumed  $2K \cdot R' \ll (K^2 + 2K \cdot R)$ . This expression corresponds to the ladder graph of Fig. 6.

We note that in this derivation there are two competing limits for the size of  $K^2 + 2K \cdot R$ : one is the infrared limit of  $2K \cdot R' \ll (K^2 + 2K \cdot R)$ , while the other is the fact that  $K^2 + 2K \cdot R$  must be sufficiently small so as to make the ladder graphs important (see Eq. (5)). It is only in special cases, such as some finite temperature examples, where both of these criteria may be simultaneously satisfied.

The particular resummation of ladder graphs indicated above is for graphs with bare internal lines and vertices. The question then arises as to how one generates such expansions when some combination of the internal lines and vertices in the ladder graphs are replaced by their effective counterparts, as in in Figs. 7–20. This question may be addressed in the same way as for bare vertices and internal lines. We first show that in the limit  $K \rightarrow 0$  the vertices and polarization tensors in Figs. 7–20 satisfy Eq. [12]. Using this result, the iteration of the partial Schwinger–Dyson equation (15) shown in Fig. 5 can then be used to generate the effective resummation of ladder graphs for the self-energy.

For example, consider the vertex of Fig. 7 with one corrected internal line:

$$\Gamma(K, P) = -i(-ig)^3 \int dR G(R)D(R+P)D(K+P+R), \quad (17)$$

where  $G(R) = 1/(R^2 - \Pi(R) + i\epsilon)$  is the full propagator. We split the two propagators  $D(R+P)D(K+P+R)$  as in Eq. [4] and use the approximation  $2K \cdot R \ll (K^2 + 2K \cdot P)$ , whereby this equation becomes

$$\Gamma(K, P) \approx -i(-ig)^3 \frac{1}{K^2 + 2K \cdot P} \int dR G(R) [D(R+P) - D(K+P+R)]. \quad (18)$$

Comparing this to the self-energy graph of Fig. 8:

$$-i\Pi(P) = -(-ig)^2 \int dR G(R)D(R+P), \quad (19)$$

we find the relation Eq. (12) is satisfied. Use of this relation in the iteration of the partial Schwinger–Dyson equation of Eq. (15) shown in Fig. 5 would lead then to a series of ladder graphs with effective propagators on the internal “vertical” lines, such as in Fig. 9. To see this, if for the first iteration we use  $\Gamma(K, R)$  of Eq. (12) with the self-energy of Fig. 8, we find

$$\begin{aligned}
-i\Pi(K) &= (ig)^2 \int dR \frac{[\Pi(R) - \Pi(K+R)]}{K^2 + 2K \cdot R} D(R)D(K+R) \\
&= -(ig)^2 \int dR \frac{D(R)D(K+R)}{K^2 + 2K \cdot R} i(-ig)^2 \int dR' \\
&\quad [G(R')D(R+R') - G(R')D(K+R+R')] \\
&= i(-ig)^4 \int dR dR' D(R)D(K+R)G(R')D(R+R')D(K+R+R'), \quad (20)
\end{aligned}$$

where we assumed  $2K \cdot R' \ll (K^2 + 2K \cdot R)$ . This corresponds to the ladder graph of Fig. 9.

We thus see that the ladder graphs may be generated by the iteration of the partial Schwinger–Dyson equation of Fig. 5. However, for completeness the full Schwinger–Dyson equation of Fig. 10 should be considered. In Ref. [28] it was shown that this equation,

$$-i\Pi(K) = ig \int dR [-ig + \Gamma(K, R)] G(R)G(K+R), \quad (21)$$

where  $G(K) = i/(K^2 - \Pi(K) + i\epsilon)$  is the full propagator, simplifies to

$$-i\Pi(K) = 2(-ig)^2 \int dR \left[ \frac{i}{K^2 + 2K \cdot R} \right] \left[ \frac{i}{R^2 - \Pi(R) + i\epsilon} \right] \quad (22)$$

if Eq. (12) hold. This simplification results from a partial cancellation of ladder graphs against non-ladder graphs. To see this cancellation explicitly, start with Eq. (21) and rewrite  $\Gamma(K, R)$  in terms of  $\Pi(K)$  using Eq. (12). Taking as an example the one-loop expression of Fig. 2, we find the first iteration of Eq. (21) gives

$$-i\Pi^{(1)}(K) = 2(-ig)^2 \int dR \left[ \frac{i}{K^2 + 2K \cdot R} \right] \left[ \frac{i}{R^2 + i\epsilon} \right], \quad (23)$$

which corresponds to the one-loop graph of Fig. 2, which is given in Eq. (22). At the next order of iteration we have two terms: one from the ladder graph of Fig. 6, given in Eq. (16), and the other from the two-loop graph of Fig. 11:

$$2(-ig)^2 \int dR dR' D(R)D(K+R)D(K+R+R')D(R')D(K+R). \quad (24)$$

When these are combined in the infrared limit one obtains

$$2(-ig)^2 \int dR \left[ \frac{i}{K^2 + 2K \cdot R} \right] \frac{i}{R^2 + i\epsilon} [-i\Pi(R)] \frac{i}{R^2 + i\epsilon}, \quad (25)$$

which is just the second term of the expansion in terms of  $\Pi$  of Eq. (22). Thus, ladder and non-ladder graphs combine to give a relatively simple expression. Further simplification is possible if we assume in Eq. (22) that the contribution of  $\Pi(R)$  to the pole in the integral is negligible, so that this expression becomes

$$-i\Pi(K) = 2(-ig)^2 \int dR \left[ \frac{i}{K^2 + 2K \cdot R} \right] \left[ \frac{i}{R^2 + i\epsilon} \right]. \quad (26)$$

This corresponds, in the infrared limit, to the one-loop graph of Fig. 2. In this case one can say that the ladder graph of Fig. 6 has canceled exactly against the non-ladder graph of Fig. 11; such cancellation in some particular examples has been found in Refs. [7,10,13].

Thus, we see that the relation of Eq. (12) between the vertex function  $\Gamma$  and self-energy  $\Pi$  is critical in two respects. Firstly, it gives an expansion of the ladder graphs in terms of the iteration of the partial Schwinger–Dyson equation of Fig. 5. Secondly, it demonstrates how ladder graphs combine with other types of terms in the full Schwinger–Dyson equation of Fig. 10 to give a relatively simple expression. The rest of the paper addresses the question of the validity of this relation at finite temperature for more complicated cases than the ones just considered. In the next three sections we express the 2, 3, and 4-point functions in a particular real-time formalism of finite temperature field theory useful for our purposes. We then show how in this formalism the relation of Eq. (12) is satisfied at finite temperature for a wide class of vertex and self-energy diagrams with corrected vertices and internal lines. We end with some brief conclusions.

#### IV. PROPAGATOR

We first consider the propagator. In real time, the propagator has  $2^2 = 4$  components, since each of the two fields can take values on either branch of the contour. Thus, the propagator can be written as a  $2 \times 2$  matrix of the form

$$D = \begin{pmatrix} D_{11} & D_{12} \\ D_{21} & D_{22} \end{pmatrix}, \quad (27)$$

where  $D_{11}$  is the propagator for fields moving along  $C_1$ ,  $D_{12}$  is the propagator for fields moving from  $C_1$  to  $C_2$ , etc. The four components are given by

$$\begin{aligned} D_{11}(x-y) &= -i\langle T(\phi(x)\phi(y)) \rangle, \\ D_{12}(x-y) &= -i\langle \phi(y)\phi(x) \rangle, \\ D_{21}(x-y) &= -i\langle \phi(x)\phi(y) \rangle, \\ D_{22}(x-y) &= -i\langle \tilde{T}(\phi(x)\phi(y)) \rangle, \end{aligned} \quad (28)$$

where  $T$  is the usual time ordering operator, and  $\tilde{T}$  is the anti-chronological time ordering operator. These four components satisfy,

$$D_{11} - D_{12} - D_{21} + D_{22} = 0 \quad (29)$$

as a consequence of the identity  $\theta(x) + \theta(-x) = 1$ .

It is more useful to write the propagator in terms of the three functions

$$\begin{aligned} D_R &= D_{11} - D_{12}, \\ D_A &= D_{11} - D_{21}, \\ D_F &= D_{11} + D_{22}. \end{aligned} \quad (30)$$

$D_R$  and  $D_A$  are the usual retarded and advanced propagators, satisfying

$$D_R(x-y) - D_A(x-y) = -i\langle [\phi(x), \phi(y)] \rangle, \quad (31)$$

and  $D_F$  is the symmetric combination

$$D_F(x - y) = -i\langle\{\phi(x), \phi(y)\}\rangle, \quad (32)$$

which satisfies in momentum space

$$D_F(P) = (1 + 2n(p_0))(D_R(P) - D_A(P)), \quad (33)$$

where

$$D_{R,A}(P) = \frac{1}{(p_0 \pm i\epsilon)^2 - \vec{p}^2 - m^2}. \quad (34)$$

Equations (29), (30) are inverted by

$$\begin{aligned} D_{11} &= \frac{1}{2}(D_F + D_A + D_R), \\ D_{12} &= \frac{1}{2}(D_F + D_A - D_R), \\ D_{21} &= \frac{1}{2}(D_F - D_A + D_R), \\ D_{22} &= \frac{1}{2}(D_F - D_A - D_R). \end{aligned} \quad (35)$$

These equations can be written in a more convenient notation as [21]

$$2D = D_R \begin{pmatrix} 1 \\ 1 \end{pmatrix} \begin{pmatrix} 1 \\ -1 \end{pmatrix} + D_A \begin{pmatrix} 1 \\ -1 \end{pmatrix} \begin{pmatrix} 1 \\ 1 \end{pmatrix} + D_F \begin{pmatrix} 1 \\ 1 \end{pmatrix} \begin{pmatrix} 1 \\ 1 \end{pmatrix} \quad (36)$$

where the outer product of the column vectors is to be taken.

Similar relations can be obtained for the polarization tensor. The polarization tensor is the 1PI two-point function and is obtained by amputating the external legs from the propagator. The Dyson equation gives

$$iD(p) = iD_0(p) + iD_0(p) (-i\Pi(p)) iD(p). \quad (37)$$

The analogues of (29) and (30) are

$$\begin{aligned} \Pi_R &= \Pi_{11} + \Pi_{12}, \\ \Pi_A &= \Pi_{11} + \Pi_{21}, \\ \Pi_F &= \Pi_{11} + \Pi_{22}, \end{aligned} \quad (38)$$

and

$$\Pi_{11} + \Pi_{12} + \Pi_{21} + \Pi_{22} = 0. \quad (39)$$

The analogues of (36) and (33) are

$$2\Pi(p) = \Pi_R(p) \begin{pmatrix} 1 \\ -1 \end{pmatrix} \begin{pmatrix} 1 \\ 1 \end{pmatrix} + \Pi_A(p) \begin{pmatrix} 1 \\ 1 \end{pmatrix} \begin{pmatrix} 1 \\ -1 \end{pmatrix} + \Pi_F(p) \begin{pmatrix} 1 \\ -1 \end{pmatrix} \begin{pmatrix} 1 \\ -1 \end{pmatrix}, \quad (40)$$

$$\Pi_F(p) = (1 + 2n(p_0)) (\Pi_R(p) - \Pi_A(p)). \quad (41)$$



One loop results for the polarization tensor are as follows. We define  $N_p = 1 + 2n(p_0)$  and  $D_R(P) = r_P$ ,  $D_A(P) = a_P$ ,  $D_F(P) = f_P$ , etc.

$$\Pi_R(K) = \frac{1}{2}ig^2 \int \frac{d^4 R}{(2\pi)^4} (a_R f_{K+R} + f_R r_{K+R}) \quad (42)$$

$$\Pi_A(K) = \frac{1}{2}ig^2 \int \frac{d^4 R}{(2\pi)^4} (r_R f_{K+R} + f_R a_{K+R}) \quad (43)$$

$$\Pi_F(K) = \frac{1}{2}ig^2 \int \frac{d^4 R}{(2\pi)^4} (r_R a_{K+R} + a_R r_{K+R} + f_R f_{K+R}) \quad (44)$$

## V. THREE-POINT FUNCTION

In the real time formalism, the three-point function has  $2^3 = 8$  components. We denote the connected functions by  $\Gamma_{abc}^C$  where  $\{a, b, c = 1, 2\}$ . In analogy to (28), they are given by the following expressions [21]:

$$\begin{aligned} \Gamma_{111}^C(x, y, z) &= \langle T(\phi(x)\phi(y)\phi(z)) \rangle, \\ \Gamma_{112}^C(x, y, z) &= \langle \phi(z) T(\phi(x)\phi(y)) \rangle, \\ \Gamma_{121}^C(x, y, z) &= \langle \phi(y) T(\phi(x)\phi(z)) \rangle, \\ \Gamma_{211}^C(x, y, z) &= \langle \phi(x) T(\phi(y)\phi(z)) \rangle, \\ \Gamma_{122}^C(x, y, z) &= \langle \tilde{T}(\phi(y)\phi(z)) \phi(x) \rangle, \\ \Gamma_{212}^C(x, y, z) &= \langle \tilde{T}(\phi(x)\phi(z)) \phi(y) \rangle, \\ \Gamma_{221}^C(x, y, z) &= \langle \tilde{T}(\phi(x)\phi(y)) \phi(z) \rangle, \\ \Gamma_{222}^C(x, y, z) &= \langle \tilde{T}(\phi(x)\phi(y)\phi(z)) \rangle. \end{aligned} \quad (45)$$

Only seven of these components are independent because of the identity

$$\sum_{a=1}^2 \sum_{b=1}^2 \sum_{c=1}^2 (-1)^{a+b+c-3} \Gamma_{abc}^C = 0 \quad (46)$$

which follows in the same way as (29) from  $\theta(x) + \theta(-x) = 1$ . The seven combinations that we use are defined as [21]

$$\begin{aligned} \Gamma_R^C &= \Gamma_{111}^C - \Gamma_{112}^C - \Gamma_{211}^C + \Gamma_{212}^C, \\ \Gamma_{Ri}^C &= \Gamma_{111}^C - \Gamma_{112}^C - \Gamma_{121}^C + \Gamma_{122}^C, \\ \Gamma_{Ro}^C &= \Gamma_{111}^C - \Gamma_{121}^C - \Gamma_{211}^C + \Gamma_{221}^C, \\ \Gamma_F^C &= \Gamma_{111}^C - \Gamma_{121}^C + \Gamma_{212}^C - \Gamma_{222}^C, \\ \Gamma_{Fi}^C &= \Gamma_{111}^C + \Gamma_{122}^C - \Gamma_{211}^C - \Gamma_{222}^C, \\ \Gamma_{Fo}^C &= \Gamma_{111}^C - \Gamma_{112}^C + \Gamma_{221}^C - \Gamma_{222}^C, \\ \Gamma_E^C &= \Gamma_{111}^C + \Gamma_{122}^C + \Gamma_{212}^C + \Gamma_{221}^C. \end{aligned} \quad (47)$$

In coordinate space we always label the first leg of the three-point function by  $x$  and call it the “incoming leg ( $i$ )”, the third leg we label by  $z$  and call it the “outgoing leg ( $o$ )”, and the second (middle) leg we label by  $y$ . Inserting the definitions (45) into (47) one finds

$$\begin{aligned}
\Gamma_R^C &= \theta_{23}\theta_{31}\langle[[\phi_2, \phi_3], \phi_1]\rangle + \theta_{21}\theta_{13}\langle[[\phi_2, \phi_1], \phi_3]\rangle, \\
\Gamma_{Ri}^C &= \theta_{12}\theta_{23}\langle[[\phi_1, \phi_2], \phi_3]\rangle + \theta_{13}\theta_{32}\langle[[\phi_1, \phi_3], \phi_2]\rangle, \\
\Gamma_{Ro}^C &= \theta_{32}\theta_{21}\langle[[\phi_3, \phi_2], \phi_1]\rangle + \theta_{31}\theta_{12}\langle[[\phi_3, \phi_1], \phi_2]\rangle, \\
\Gamma_F^C &= \theta_{12}\theta_{23}\langle\{[\phi_1, \phi_2], \phi_3\}\rangle + \theta_{32}\theta_{21}\langle\{[\phi_3, \phi_2], \phi_1\}\rangle + \theta_{12}\theta_{32}\langle\{[\phi_3, \phi_1], \phi_2\}\rangle, \\
\Gamma_{Fi}^C &= \theta_{21}\theta_{13}\langle\{[\phi_2, \phi_1], \phi_3\}\rangle + \theta_{31}\theta_{12}\langle\{[\phi_3, \phi_1], \phi_2\}\rangle + \theta_{21}\theta_{31}\langle\{[\phi_2, \phi_3], \phi_1\}\rangle, \\
\Gamma_{Fo}^C &= \theta_{23}\theta_{31}\langle\{[\phi_2, \phi_3], \phi_1\}\rangle + \theta_{13}\theta_{32}\langle\{[\phi_1, \phi_3], \phi_2\}\rangle + \theta_{13}\theta_{23}\langle\{[\phi_1, \phi_2], \phi_3\}\rangle, \\
\Gamma_E^C &= \theta_{13}\theta_{23}\langle\{\{\phi_1, \phi_2\}, \phi_3\}\rangle + \theta_{21}\theta_{31}\langle\{\{\phi_2, \phi_3\}, \phi_1\}\rangle + \theta_{12}\theta_{32}\langle\{\{\phi_1, \phi_3\}, \phi_2\}\rangle,
\end{aligned} \tag{48}$$

where we have used the obvious shorthands  $\phi_1 \equiv \phi(x)$ ,  $\phi_2 \equiv \phi(y)$ ,  $\phi_3 \equiv \phi(z)$ , and  $\theta_{12} \equiv \theta(x_0 - y_0)$ , etc. The first three are the retarded three-point functions;  $\Gamma_{Ri}^C$  is retarded with respect to  $x_0$ ,  $\Gamma_{Ro}^C$  is retarded with respect to  $z_0$ , and  $\Gamma_R^C$  is retarded with respect to  $y_0$ .

When doing calculations one is usually interested in the 1PI vertex functions which are obtained from the connected functions by truncating external legs. We will denote 1PI vertex functions by  $\Gamma$ . We can write  $\Gamma$  as a tensor of the form

$$\Gamma = \begin{pmatrix} a \\ b \end{pmatrix} \begin{pmatrix} c \\ d \end{pmatrix} \begin{pmatrix} e \\ f \end{pmatrix} \tag{49}$$

where the outer product of the column vectors is to be taken. For the 1PI functions the analogues of (46) and (47) are,

$$\sum_{a=1}^2 \sum_{b=1}^2 \sum_{c=1}^2 \Gamma_{abc} = a + b + c + d + e + f = 0, \tag{50}$$

and,

$$\begin{aligned}
\Gamma_R &= \Gamma_{111} + \Gamma_{112} + \Gamma_{211} + \Gamma_{212} = \frac{1}{2}(a+b)(c-d)(e+f), \\
\Gamma_{Ri} &= \Gamma_{111} + \Gamma_{112} + \Gamma_{121} + \Gamma_{122} = \frac{1}{2}(a-b)(c+d)(e+f), \\
\Gamma_{Ro} &= \Gamma_{111} + \Gamma_{121} + \Gamma_{211} + \Gamma_{221} = \frac{1}{2}(a+b)(c+d)(e-f), \\
\Gamma_F &= \Gamma_{111} + \Gamma_{121} + \Gamma_{212} + \Gamma_{222} = \frac{1}{2}(a-b)(c+d)(e-f), \\
\Gamma_{Fi} &= \Gamma_{111} + \Gamma_{122} + \Gamma_{211} + \Gamma_{222} = \frac{1}{2}(a+b)(c-d)(e-f), \\
\Gamma_{Fo} &= \Gamma_{111} + \Gamma_{112} + \Gamma_{221} + \Gamma_{222} = \frac{1}{2}(a-b)(c-d)(e+f), \\
\Gamma_E &= \Gamma_{111} + \Gamma_{122} + \Gamma_{212} + \Gamma_{221} = \frac{1}{2}(a-b)(c-d)(e-f).
\end{aligned} \tag{51}$$

The 1PI vertex functions  $\Gamma(P_1, P_2, P_3)$  are related to the connected vertex functions  $\Gamma(P_1, P_2, P_3)$  as follows:

$$\begin{aligned}
\Gamma_R &= i^3 a_1 r_2 a_3 \Gamma_R \\
\Gamma_{Ri} &= i^3 r_1 a_2 a_3 \Gamma_{Ri}
\end{aligned}$$

$$\begin{aligned}
\Gamma_{Ro} &= i^3 a_1 a_2 r_3 \Gamma_{Ro} \\
\Gamma_F &= i^3 [r_1 a_2 f_3 \Gamma_{Ri} + f_1 a_2 r_3 \Gamma_{Ro} + r_1 a_2 r_3 \Gamma_F] \\
\Gamma_{Fi} &= i^3 [a_1 r_2 f_3 \Gamma_R + a_1 f_2 r_3 \Gamma_{Ro} + a_1 r_2 r_3 \Gamma_{Fi}] \\
\Gamma_{Fo} &= i^3 [r_1 f_2 a_3 \Gamma_{Ri} + f_1 r_2 a_3 \Gamma_R + r_1 r_2 a_3 \Gamma_{Fo}] \\
\Gamma_E &= i^3 [f_1 r_2 f_3 \Gamma_R + r_1 f_2 f_3 \Gamma_{Ri} + f_1 f_2 r_3 \Gamma_{Ro} \\
&\quad + r_1 f_2 r_3 \Gamma_F + f_1 r_2 r_3 \Gamma_{Fi} + r_1 r_2 f_3 \Gamma_{Fo} + r_1 r_2 r_3 \Gamma_E]
\end{aligned}$$

For calculational purposes, it is useful to obtain a decomposition of the 1PI three-point function in terms of the seven functions (51), in analogy to (36) for the two-point function. Inverting (51) we obtain

$$\begin{aligned}
4\Gamma &= \Gamma_R \begin{pmatrix} 1 \\ 1 \end{pmatrix} \begin{pmatrix} 1 \\ -1 \end{pmatrix} \begin{pmatrix} 1 \\ 1 \end{pmatrix} + \Gamma_{Ri} \begin{pmatrix} 1 \\ -1 \end{pmatrix} \begin{pmatrix} 1 \\ 1 \end{pmatrix} \begin{pmatrix} 1 \\ 1 \end{pmatrix} \\
&\quad + \Gamma_{Ro} \begin{pmatrix} 1 \\ 1 \end{pmatrix} \begin{pmatrix} 1 \\ 1 \end{pmatrix} \begin{pmatrix} 1 \\ -1 \end{pmatrix} + \Gamma_F \begin{pmatrix} 1 \\ -1 \end{pmatrix} \begin{pmatrix} 1 \\ 1 \end{pmatrix} \begin{pmatrix} 1 \\ -1 \end{pmatrix} \\
&\quad + \Gamma_{Fi} \begin{pmatrix} 1 \\ 1 \end{pmatrix} \begin{pmatrix} 1 \\ -1 \end{pmatrix} \begin{pmatrix} 1 \\ -1 \end{pmatrix} + \Gamma_{Fo} \begin{pmatrix} 1 \\ -1 \end{pmatrix} \begin{pmatrix} 1 \\ -1 \end{pmatrix} \begin{pmatrix} 1 \\ 1 \end{pmatrix} \\
&\quad + \Gamma_E \begin{pmatrix} 1 \\ -1 \end{pmatrix} \begin{pmatrix} 1 \\ -1 \end{pmatrix} \begin{pmatrix} 1 \\ -1 \end{pmatrix}.
\end{aligned} \tag{52}$$

One loop expressions for the three point functions are as follows. We use  $P_- = P - K/2$ ,  $P_+ = -(P + K/2)$ ,  $P_1 = P + R - K/2$  and  $P_3 = -(P + R + K/2)$  (see Fig. 12).

$$\begin{aligned}
\Gamma_R(P_-, K, P_+) &= \frac{1}{2} g^3 \int \frac{d^4 R}{(2\pi)^4} (f_R a_1 a_3 + r_R f_1 a_3 + a_R a_1 f_3) \\
\Gamma_{Ri}(P_-, K, P_+) &= \frac{1}{2} g^3 \int \frac{d^4 R}{(2\pi)^4} (f_R r_1 a_3 + a_R f_1 r_3 + a_R r_1 f_3) \\
\Gamma_{Ro}(P_-, K, P_+) &= \frac{1}{2} g^3 \int \frac{d^4 R}{(2\pi)^4} (f_R a_1 r_3 + r_R f_1 r_3 + r_R r_1 f_3) \\
\Gamma_F(P_-, K, P_+) &= \frac{1}{2} g^3 \int \frac{d^4 R}{(2\pi)^4} (f_R (f_1 r_3 + f_3 r_1) + a_R a_3 r_1 + r_R r_3 a_1) \\
\Gamma_{Fi}(P_-, K, P_+) &= \frac{1}{2} g^3 \int \frac{d^4 R}{(2\pi)^4} (f_3 (r_R f_1 + f_R a_1) + r_R r_1 r_3 + a_R a_1 a_3) \\
\Gamma_{Fo}(P_-, K, P_+) &= \frac{1}{2} g^3 \int \frac{d^4 R}{(2\pi)^4} (f_1 (f_R a_3 + a_R f_3) + r_R a_3 a_1 + a_R r_3 r_1)
\end{aligned} \tag{53}$$

We are interested in the infra-red limit  $K \rightarrow 0$ . We use the splitting identity of the form

$$D_1 D_3 = \frac{1}{P_3^2 - P_1^2} (D_1 - D_3) = \frac{1}{2K \cdot (P + R)} (D_1 - D_3) \approx \frac{1}{2K \cdot P} (D_1 - D_3) \tag{54}$$

where we take the limit  $R \rightarrow 0$  to study the infra-red limit. This identity allows us to rewrite the one-loop three point vertex in terms of a difference in one-loop two point functions. We will work with the vertex function that is retarded with respect to the middle leg and obtain,

$$\Gamma_R(P_-, K, P_+) = -\frac{ig}{2P \cdot K}(\Pi_A(P_-) - \Pi_A(P_+)), \quad (55)$$

which is another form of (12) that is valid at finite temperature.

## VI. FOUR-POINT FUNCTION

The 1PI four-point function forms a 16 component tensor which we can write as the outer product of four two component vectors,

$$M = \begin{pmatrix} a \\ b \end{pmatrix} \begin{pmatrix} c \\ d \end{pmatrix} \begin{pmatrix} e \\ f \end{pmatrix} \begin{pmatrix} g \\ h \end{pmatrix} \quad (56)$$

Then the retarded 1PI four-point functions are given by

$$\begin{aligned} M_{R1} &= M_{1111} + M_{1112} + M_{1121} + M_{1211} + M_{1122} + M_{1212} + M_{1221} + M_{1222} \\ &= \frac{1}{2}(a-b)(c+d)(e+f)(g+h) \\ M_{R2} &= M_{1111} + M_{1112} + M_{1121} + M_{2111} + M_{1122} + M_{2112} + M_{2121} + M_{2122} \\ &= \frac{1}{2}(a+b)(c-d)(e+f)(g+h) \\ M_{R3} &= M_{1111} + M_{1112} + M_{2111} + M_{1211} + M_{2112} + M_{1212} + M_{2211} + M_{2212} \\ &= \frac{1}{2}(a+b)(c+d)(e-f)(g+h) \\ M_{R4} &= M_{1111} + M_{2111} + M_{1121} + M_{1211} + M_{2121} + M_{2211} + M_{1221} + M_{2221} \\ &= \frac{1}{2}(a+b)(c+d)(e+f)(g-h) \end{aligned} \quad (57)$$

where we have used the relation

$$\sum_{a,b,c,d=1}^2 M_{abcd} = 0. \quad (58)$$

The other combinations we will need are,

$$\begin{aligned} M_A &= \frac{1}{2}(a+b)(c+d)(e-f)(g-h) \\ M_B &= \frac{1}{2}(a-b)(c+d)(e-f)(g+h) \\ M_C &= \frac{1}{2}(a+b)(c-d)(e-f)(g+h) \\ M_D &= \frac{1}{2}(a+b)(c-d)(e+f)(g-h) \\ M_E &= \frac{1}{2}(a-b)(c-d)(e+f)(g+h) \\ M_F &= \frac{1}{2}(a-b)(c+d)(e+f)(g-h) \end{aligned} \quad (59)$$

The one loop results are,

$$\begin{aligned}
M_{R1} &= \frac{1}{2}g^4 \int \frac{d^4 R}{(2\pi)^4} (f_R a_1 r_3 a_4 + r_R f_1 r_3 a_4 + r_R r_1 f_3 a_4 + a_R a_1 r_3 f_4) \\
M_{R2} &= \frac{1}{2}g^4 \int \frac{d^4 R}{(2\pi)^4} (f_R a_1 a_3 a_4 + r_R f_1 a_3 a_4 + a_R a_1 f_3 r_4 + a_R a_1 a_3 f_4) \\
M_{R3} &= \frac{1}{2}g^4 \int \frac{d^4 R}{(2\pi)^4} (f_R r_1 a_3 a_4 + a_R f_1 r_3 r_4 + a_R r_1 f_3 r_4 + a_R r_1 a_3 f_4) \\
M_{R4} &= \frac{1}{2}g^4 \int \frac{d^4 R}{(2\pi)^4} (f_R a_1 r_3 r_4 + r_R f_1 r_3 r_4 + r_R r_1 f_3 r_4 + r_R r_1 a_3 f_4) \\
M_A &= \frac{1}{2}g^4 \int \frac{d^4 R}{(2\pi)^4} (r_R a_1 r_3 r_4 + a_R r_1 a_3 a_4 + f_R (f_1 r_3 r_4 + r_1 f_3 r_4 + r_1 a_3 f_4)) \\
M_B &= \frac{1}{2}g^4 \int \frac{d^4 R}{(2\pi)^4} (r_R a_1 r_3 a_4 + a_R r_1 a_3 r_4 + f_R f_1 r_3 a_4 + a_R f_1 r_3 f_4 + f_R r_1 f_3 a_4 + a_R r_1 f_3 f_4) \\
M_C &= \frac{1}{2}g^4 \int \frac{d^4 R}{(2\pi)^4} (a_R r_1 r_3 r_4 + r_R a_1 a_3 a_4 + f_1 (a_R f_3 r_4 + f_R a_3 a_4 + a_R a_3 f_4)) \\
M_D &= \frac{1}{2}g^4 \int \frac{d^4 R}{(2\pi)^4} (r_R r_1 r_3 r_4 + a_R a_1 a_3 a_4 + r_R f_1 f_3 r_4 + f_R a_1 f_3 r_4 + r_R f_1 a_3 f_4 + f_R a_1 a_3 f_4) \\
M_E &= \frac{1}{2}g^4 \int \frac{d^4 R}{(2\pi)^4} (r_R r_1 r_3 a_4 + a_R a_1 a_3 r_4 + f_3 (r_R f_1 a_4 + f_R a_1 a_4 + a_R a_1 f_4)) \\
M_F &= \frac{1}{2}g^4 \int \frac{d^4 R}{(2\pi)^4} (a_R a_1 r_3 a_4 + r_R r_1 a_3 r_4 + f_4 (f_R a_1 r_3 + r_R f_1 r_3 + r_R r_1 f_3) f_4)
\end{aligned} \tag{60}$$

Variables are defined as in Fig. 13.

Using (53) and (54) we obtain the splitting relations that we will need:

$$\begin{aligned}
M_{R2}(P_-, K, P_3, R) &= \frac{g}{2P \cdot K} [\Gamma_R(P_-, -P_1, R) - \Gamma_{Ri}(-P_+, P_3, R)] \\
M_{R2}(P_1, K, P_+, -R) &= \frac{g}{2P \cdot K} [\Gamma_R(P_1, -P_-, -R) + \Gamma_R^*(-P_+, P_3, R)]
\end{aligned} \tag{62}$$

## VII. FIVE-POINT FUNCTION

The 1PI five-point function forms a 32 component tensor which we can write as the outer product of five two component vectors,

$$M = \begin{pmatrix} a \\ b \end{pmatrix} \begin{pmatrix} c \\ d \end{pmatrix} \begin{pmatrix} e \\ f \end{pmatrix} \begin{pmatrix} g \\ h \end{pmatrix} \begin{pmatrix} i \\ j \end{pmatrix} \tag{63}$$

The vertices that we need are given by,

$$\begin{aligned}
C_{R2} &= \frac{1}{2}(a+b)(c-d)(e+f)(g+h)(i+j) \\
C_\alpha &= \frac{1}{2}(a+b)(c-d)(e+f)(g-h)(i+j) \\
C_\beta &= \frac{1}{2}(a+b)(c-d)(e+f)(g+h)(i-j)
\end{aligned}$$

The one loop results are given by,

$$\begin{aligned}
C_{R2} &= \frac{1}{2}g^5 \int \frac{d^4L}{(2\pi)^4} [r_L r_L f_1 a_3 r_{R+L} + a_L r_L a_1 a_3 f_{R+L} + a_L f_L a_1 a_3 a_{R+L} + a_L a_L a_1 f_3 a_{R+L} \\
&\quad + r_L f_L a_1 a_3 r_{R+L}] \\
C_\alpha &= \frac{1}{2}g^5 \int \frac{d^4L}{(2\pi)^4} [r_L a_L r_1 r_3 r_{R+L} + a_L r_L f_1 f_3 r_{R+L} + r_L f_L f_1 a_3 r_{R+L} + a_L r_L a_1 a_3 a_{R+L} \\
&\quad + a_L f_L a_1 a_3 f_{R+L} + a_l a_l a_1 f_3 f_{R+L} + f_l f_l a_1 a_3 r_{R+L} + a_L f_L a_1 f_3 r_{R+L}] \\
C_\beta &= \frac{1}{2}g^5 \int \frac{d^4L}{(2\pi)^4} [r_L a_L r_1 r_3 a_{R+L} + r_L r_L f_1 a_3 f_{R+L} + r_L a_L f_1 f_3 a_{R+L} + r_L f_L f_1 a_3 a_{R+L} \\
&\quad + r_L a_L a_1 a_3 r_{R+L} + r_L f_L a_1 a_3 f_{R+L} + f_L f_L a_1 a_3 a_{R+L} + a_L f_L a_1 f_3 a_{R+L}]
\end{aligned}$$

Variables are defined as in Fig. 14.

Using (54) and (61) we obtain, in the infra-red limit, the relations,

$$\begin{aligned}
C_{R2}(P_-, K, P_+, R, -R) &= -\frac{g}{2P \cdot K} [M_{R2}^*(-P_-, P_-, -R, R) + M_{R2}(P_+, -P_+, -R, R)] \\
C_\alpha(P_-, K, P_+, R, -R) &= \frac{g}{2P \cdot K} [M_C^*(-P_-, P_-, -R, R) - M_D(P_+, -P_+, -R, R)] \\
C_\beta(P_-, K, P_+, R, -R) &= \frac{g}{2P \cdot K} [M_D^*(-P_-, P_-, -R, R) - M_C(P_+, -P_+, -R, R)] \quad (64)
\end{aligned}$$

## VIII. LADDER RESUMMATION AND CANCELLATION AT FINITE TEMPERATURE

We earlier discussed at zero temperature how the full Schwinger–Dyson equation of Fig. 10 simplifies to Eq. (22) when the relation of Eq. (12) holds between the vertex and self-energy function. In this section we generalize this result to finite temperature. In this formalism the full Schwinger–Dyson equation has the form

$$\begin{aligned}
\Pi_R(K) &= \frac{1}{2}ig^2 \int \frac{d^4R}{(2\pi)^4} [ \Delta_A(R)\Delta_F(K+R) + \Delta_F(R)\Delta_R(K+R) \\
&\quad + i\{-\Gamma_{Ri}^*(-K-R, K, R)\Delta_F(R)\Delta_R(K+R) \\
&\quad - \Gamma_{Ro}^*(-K-R, K, R)\Delta_A(R)\Delta_F(K+R) \\
&\quad + \Gamma_F^*(-K-R, K, R)\Delta_A(R)\Delta_R(K+R)\}] \quad (65)
\end{aligned}$$

where the propagators are full ones. We rewrite this expression by using the splitting relations for the three point vertices, analogous to Eq. (55). We obtain

$$\begin{aligned}
\Gamma_{Ri}^*(-K-R, K, R) &= -\frac{ig}{K^2 + 2K \cdot R} (\Pi_R(K+R) - \Pi_R(R)) \\
\Gamma_{Ro}^*(-K-R, K, R) &= -\frac{ig}{K^2 + 2K \cdot R} (\Pi_A(K+R) - \Pi_A(R)) \\
\Gamma_F^*(-K-R, K, R) &= \frac{ig}{K^2 + 2K \cdot R} (\Pi_F(K+R) - \Pi_F(R)) \quad (66)
\end{aligned}$$

Splitting the propagators gives

$$\begin{aligned}\Delta_R(R)\Delta_R(K+R) &= \frac{\Delta_R(R) - \Delta_R(K+R)}{K^2 + 2K \cdot R + \Pi_R(R) - \Pi_R(K+R)} \\ \Delta_A(R)\Delta_R(K+R) &= \frac{\Delta_A(R) - \Delta_R(K+R)}{K^2 + 2K \cdot R + \Pi_A(R) - \Pi_R(K+R)}\end{aligned}\quad (67)$$

and substituting Eq. (66) and Eq. (67) into Eq. (65) we obtain

$$\Pi_R(K) = ig^2 \int \frac{d^4 R}{(2\pi)^4} \frac{\Delta_F(R)}{K^2 + 2K \cdot R}, \quad (68)$$

which is the desired result.

As a specific example of this type of simplification, we consider the set of diagrams shown in Figs. 2, 6, and 11, which we call respectively  $\Pi^{(1)}$ ,  $\Pi^{(2)}$ , and  $\Pi^{(3)}$ . The diagram of Fig. (2) is given after splitting the propagators as

$$\Pi_R^{(1)}(K) = ig^2 \int \frac{d^4 R}{(2\pi)^4} \frac{f_R}{k^2 + 2K \cdot R} \quad (69)$$

The diagram of Fig. 11 is given by the integral

$$\begin{aligned}\Pi_R^{(2)}(K) &= \frac{1}{4}g^4 \int \frac{d^4 R}{(2\pi)^4} \int \frac{d^4 R'}{(2\pi)^4} \\ &\quad [r_{R+K}a_R(a_{R+R'}f_Rf_{R'} + a_{R+R'}r_Rr_{R'} + r_{R+R'}r_Ra_{R'} + f_{R+R'}r_Rf_{R'} + f_{R+R'}f_Rr_{R'}) \\ &\quad + r_{R+K}f_R(r_{R+R'}r_Rf_{R'} + r_{R+R'}f_Rr_{R'} + a_{R+R'}f_Ra_{R'} + f_{R+R'}r_Ra_{R'}) \\ &\quad + f_{R+K}a_R(a_{R+R'}a_Rf_{R'} + f_{R+R'}a_Rr_{R'}) + f_{R+K}f_R(r_{R+R'}a_Rr_{R'} + a_{R+R'}a_Ra_{R'}) \\ &\quad + a_{R+K}r_R(r_{R+R'}a_Rr_{R'} + a_{R+R'}a_Ra_{R'})]\end{aligned}\quad (70)$$

We split pairs of propagators of the form  $D_R D_{R+K}$  and rewrite the result by extracting polarization tensors from the factors involving integrals over  $R'$ . There are two pieces. The first does not involve propagators that depend on  $R+K$  and is given by,

$$\begin{aligned}&\frac{ig^2}{2} \int \frac{d^4 R}{(2\pi)^4} \frac{1}{K^2 + 2K \cdot R} [a_R f_R \Pi_A(R) + a_R r_R \Pi_F(R) + f_R r_R \Pi_R(R)] \\ &= \frac{ig^2}{2} \int \frac{d^4 R}{(2\pi)^4} \frac{1}{K^2 + 2K \cdot R} N_R (r_R^2 \Pi_R(R) - a_R^2 \Pi_A(R))\end{aligned}\quad (71)$$

Multiplying this result by two, as indicated by the Schwinger-Dyson equation, and combining with the zeroth order result (69) gives,

$$ig^2 \int \frac{d^4 R}{(2\pi)^4} \frac{1}{K^2 + 2K \cdot R} N_R [r_R + r_R^2 \Pi_R(R) - (a_R + a_R^2 \Pi_R(R))]\quad (72)$$

which is the first two terms in the expansion of Eq. (68).

Next we show that the second piece of  $\Pi_R^{(2)}$  cancels with  $\Pi_R^{(3)}$ . The piece of  $\Pi_R^{(2)}$  that contains the propagator  $D_{R+K}$  is given by (with the factor of two from the Schwinger-Dyson equation),

$$-ig^2 \int \frac{d^4 R}{(2\pi)^4} \frac{1}{K^2 + 2K \cdot R} (r_{R+K} a_R \Pi_F(R) + r_{R+K} f_R \Pi_R(R) + f_{R+K} a_R \Pi_A(R)) \quad (73)$$

We compare this result with the expression for the diagram Fig. 6,

$$\begin{aligned} \Pi_R^{(3)} = & -\frac{1}{4}g^4 \int \frac{d^4 R}{(2\pi)^4} \int \frac{d^4 R'}{(2\pi)^4} \\ & [ a_R r_{R+K} (r_{K+R+R'} r_{R+R'} a_{R'} + r_{K+R+R'} f_{R+R'} f_{R'} + f_{K+R+R'} a_{R+R'} f_{R'} + a_{K+R+R'} r_{R'} a_{R+R'}) \\ & + a_R f_{R+K} (a_{K+R+R'} a_{R+R'} f_{R'} + r_{K+R+R'} f_{R+R'} r_{R'} + f_{K+R+R'} a_{R+R'} r_{R'}) \\ & + f_R r_{R+K} (r_{K+R+R'} r_{R+R'} f_{R'} + r_{K+R+R'} f_{R+R'} a_{R'} + f_{K+R+R'} a_{R+R'} a_{R'}) ] \end{aligned} \quad (74)$$

We do the variable shift  $R \rightarrow -(R+K)$  on the second term, and split pairs of propagators of the form  $D_{K+R+R'} D_{R+R'}$ . This splitting introduces a denominator  $K^2 + 2K \cdot (R+R')$ . We take the infrared limit  $K^2 + 2K \cdot (R+R') \rightarrow K^2 + 2K \cdot R$  and extract polarization tensors as before to obtain,

$$ig^2 \int \frac{d^4 R}{(2\pi)^4} \frac{1}{K^2 + 2K \cdot R} (f_R r_{R+K} \Pi_R(R) + f_{R+K} a_R \Pi_A(R) + a_R r_{R+K} \Pi_F(R)) \quad (75)$$

which cancels with Eq. (73).

## IX. LADDER RESUMMATIONS

In this section we show in the infrared limit that a wide class of vertices and polarization tensors (Figs. 7–20) with internal vertex and self energy corrections satisfy Eq. (55). As discussed earlier, the significance of this result is twofold. First of all, it allows us to construct an expansion of ladder graphs in terms of the iterative solution to a partial Schwinger–Dyson equation. Secondly, it can be used to show that the solution to the Schwinger–Dyson equation for the full self-energy simplifies considerably when these ladder graphs are combined with certain non-ladder graphs.

We start with Fig. 7. The vertex is given by

$$\Gamma_{abc}(P_-, K, P_+) = i^4 (-ig)^3 \int \frac{d^4 R}{(2\pi)^4} (\tau_3 D(R))_{cd} (-i\Pi_{de}(R)) (D(R)\tau_3)_{ea} D_{ab}(P_1) (D(P_3)\tau_3)_{cb} \quad (76)$$

We use (36) and (40) to write the propagators and polarization tensors as the outer products of column vectors and expand indices according to the rules given in [22], [27]. We take only those terms that we need to get  $\Gamma_R$  (47). The result is,

$$\begin{aligned} \Gamma_R(P_-, K, P_+) = & \frac{1}{2}g^3 \int \frac{d^4 R}{(2\pi)^4} [\Pi_R(R) r_R a_3 (r_R f_1 + f_R a_1) + \Pi_A(R) a_R a_1 (f_R a_3 + a_R f_3) \\ & + \Pi_F(R) a_R r_R a_1 a_3] \end{aligned}$$

We split products of propagators of the form  $S_1 S_3$  to obtain,



$$\begin{aligned}\Gamma_R(P_-, K, P_+) &= \frac{1}{2}g^3 \frac{1}{2P \cdot K} \int \frac{d^4 R}{(2\pi)^4} \{ \Pi_R(R) [r_R^2 f_1 + r_R f_R (a_1 - a_3)] \\ &\quad + \Pi_A[a_R f_R (a_1 - a_3) - a_R^2 f_3] + \Pi_F a_R r_R (a_1 - a_3) \} \end{aligned} \quad (77)$$

To rewrite this equation we compare with the expression for the polarization tensor in Fig. 8. The result is,

$$\begin{aligned}\Pi_R(K) &= \frac{1}{2}ig^2 \int \frac{d^4 R}{(2\pi)^4} [\Pi_A(R)(r_{R+K} a_R f_R + f_{R+K} a_R a_R) + \Pi_R(R) r_{R+K} f_R r_R \\ &\quad + \Pi_F(R) r_{R+K} a_R r_R] \end{aligned} \quad (78)$$

Comparison shows that (77), (78) satisfy (55) as required.

Next we consider Fig. 15. The three vertex diagrams give respectively,

$$\begin{aligned}\Gamma_R(P_-, K, P_+) &= \frac{i}{2}g^2 \int \frac{d^4 R}{(2\pi)^4} [\Gamma_{Fi}(P_1, K, P_3) a_1 r_3 a_R + \Gamma_{Fo}(P_1, K, P_3) r_1 a_3 r_R \\ &\quad + \Gamma_R(P_1, K, P_3) (a_1 a_R f_3 + a_1 f_R a_3 + f_1 r_R a_3)] \\ &\quad + \frac{1}{2}g^3 \int \frac{d^4 R}{(2\pi)^4} [\Pi_R(P_1) r_1 f_1 a_3 r_R + \Pi_F(P_1) r_1 a_1 r_R a_3 \\ &\quad + \Pi_A(P_1) a_1 (a_3 r_R f_1 + a_3 f_R a_1 + f_3 a_R a_1)] \\ &\quad + \frac{1}{2}g^3 \int \frac{d^4 R}{(2\pi)^4} [\Pi_R(P_3) f_3 r_3 a_R a_1 + \Pi_F(P_3) a_3 r_3 a_1 a_R \\ &\quad + \Pi_A(P_3) a_3 (a_1 a_R f_3 + a_1 f_R a_3 + f_1 r_R a_3)] \end{aligned} \quad (79)$$

We rewrite this expression as follows. We note that the terms proportional to  $\Gamma_{Fi}$  and  $\Gamma_{Fo}$  give zero after integration (assuming no poles in the vertices themselves). We rewrite the term proportional to  $\Gamma_R$  by using the relation (55) that we are trying to verify. Finally, for the terms that contain a polarization tensor, we split products of propagators of the form  $S_1 S_3$ . We give the result below.

$$\begin{aligned}\Gamma_R(P_-, K, P_+) &= \frac{1}{2}g^3 \frac{1}{2P \cdot K} \int \frac{d^4 R}{(2\pi)^4} [\Pi_A(P_1) (r_R a_1 f_1 + f_R a_1 a_1) - \Pi_A(P_3) (a_R a_3 f_3 + f_R a_3 a_3) \\ &\quad + \Pi_R(P_1) r_R r_1 f_1 - \Pi_R(P_3) a_R r_3 f_3 + \Pi_F(P_1) r_R r_1 a_1 - \Pi_F(P_3) a_R r_3 a_3] \end{aligned} \quad (80)$$

The expression for the polarization tensor of Fig. 16 is,

$$\Pi_A(P_-) = \frac{1}{2}ig^2 \int \frac{d^4 R}{(2\pi)^4} [\Pi_F(P_1) r_R r_1 a_1 + \Pi_R(P_1) r_R r_1 f_1 + \Pi_A(P_1) a_1 (r_R f_1 + f_R a_1)] \quad (81)$$

Comparison shows that (55) is satisfied.

Next we consider the vertices in figure Fig. 17. From left to right, top to bottom, we obtain for the first diagram

$$\begin{aligned}\Gamma_R(P_-, K, P_+) &= \frac{i}{2}g^2 \int \frac{d^4 R}{(2\pi)^4} [\Gamma_{Ri}(-P_1, P_-, R) a_1 (a_R f_3 + f_R a_3) + \Gamma_{Ro}(-P_1, P_-, R) r_R f_1 a_3 \\ &\quad + \Gamma_F(-P_1, P_-, R) r_R a_1 a_3] \end{aligned} \quad (82)$$

Splitting the propagators of the form  $S_1 S_3$  using (54) we have,

$$\begin{aligned}\Gamma_R(P_-, K, P_+) &= \frac{i}{2}g^2 \frac{1}{2P \cdot K} \int \frac{d^4 R}{(2\pi)^4} [\Gamma_{Ri}(-P_1, P_-, R)(f_R(a_1 - a_3) - a_R f_3) \\ &\quad + \Gamma_{Ro}(-P_1, P_-, R)r_R f_1 + \Gamma_F(-P_1, P_-, R)r_R a_1]\end{aligned}\quad (83)$$

The second diagram yields

$$\begin{aligned}\Gamma_R(P_-, K, P_+) &= \frac{i}{2}g^2 \int \frac{d^4 R}{(2\pi)^4} [\Gamma_R(P_+, -P_3, -R)a_3(r_R f_1 + f_R a_1) \\ &\quad + \Gamma_{Ro}(P_+, -P_3, -R)a_R a_1 f_3 + \Gamma_{Fi}(P_+, -P_3, -R)a_R a_1 a_3]\end{aligned}\quad (84)$$

and splitting propagators we obtain,

$$\begin{aligned}\Gamma_R(P_-, K, P_+) &= \frac{i}{2}g^2 \frac{1}{2P \cdot K} \int \frac{d^4 R}{(2\pi)^4} [\Gamma_R(P_+, -P_3, -R)(r_R f_1 + f_R(a_1 - a_3)) \\ &\quad - \Gamma_{Ro}(P_+, -P_3, -R)a_R f_3 - \Gamma_{Fi}(P_+, -P_3, -R)a_R a_3]\end{aligned}\quad (85)$$

The third diagram of Fig. 17 gives

$$\begin{aligned}\Gamma_R(P_-, K, P_+) &= \frac{i}{2}g \int \frac{d^4 R}{(2\pi)^4} [M_{R2}(P_-, K, P_3, R)(f_R a_3 + f_3 a_R) \\ &\quad + M_C(P_-, K, P_3, R)a_R r_3 + M_D(P_-, K, P_3, R)r_R a_3]\end{aligned}\quad (86)$$

We drop the last two terms since they give zero by contour integration and rewrite the first term using the relation (62) which gives,

$$\Gamma_R(P_-, K, P_+) = \frac{i}{2}g^2 \frac{1}{2P \cdot K} \int \frac{d^4 R}{(2\pi)^4} [\Gamma_R(P_-, -P_1, R) - \Gamma_{Ri}(-P_+, P_3, R)](f_R a_3 + f_3 a_R)\quad (87)$$

Finally, the fourth diagram of Fig. 17 yields

$$\begin{aligned}\Gamma_R(P_-, K, P_+) &= \frac{i}{2}g \int \frac{d^4 R}{(2\pi)^4} [M_{R2}(P_1, K, P_+, -R)(f_R a_1 + f_1 r_R) \\ &\quad + M_C(P_1, K, P_+, -R)r_R r_1 + M_D(P_1, K, P_+, -R)a_R a_1].\end{aligned}\quad (88)$$

Dropping the terms that give zero after integration and using the relation (62) gives,

$$\Gamma_R(P_-, K, P_+) = \frac{i}{2}g^2 \frac{1}{2P \cdot K} \int \frac{d^4 R}{(2\pi)^4} [\Gamma_R(P_1, -P_-, -R) + \Gamma_R^*(-P_+, P_3, R)](f_R a_1 + f_1 r_R)\quad (89)$$

We need to compare with the expressions for the polarization tensors given in Fig. 18. We have,

$$\begin{aligned}\Pi_A(P_-) = & -\frac{1}{2}g \int \frac{d^4R}{(2\pi)^4} [\Gamma_R(P_1, -P_-, -R)(f_R a_1 + r_R f_1) + \Gamma_{Ri}(-P_1, P_-, R)f_R a_1 \\ & + \Gamma_{Ro}(-P_1, P_-, R)r_R f_1 + \Gamma_F(-P_1, P_-, R)r_R a_1]\end{aligned}\quad (90)$$

$$\begin{aligned}\Pi_A(P_+) = & -\frac{1}{2}g \int \frac{d^4R}{(2\pi)^4} [\Gamma_{Ri}(-P_+, P_3, R)(f_R a_3 + a_R f_3) + \Gamma_R(P_+, -P_3, -R)f_R a_3 \\ & + \Gamma_{Ro}(P_+, -P_3, -R)a_R f_3 + \Gamma_{Fi}(P_+, -P_3, -R)a_R a_3]\end{aligned}\quad (91)$$

Using  $\Gamma_{Rx}(\{P_i\}) = -\Gamma_{Rx}^*(-\{P_i\})$  and  $\Gamma_{Fx}(\{P_i\}) = \Gamma_{Fx}^*(-\{P_i\})$ , where  $\{x, i\} = \{1, 2, 3\}$ , we find that Eq. (55) is satisfied.

Lastly we look at Fig. 19, which is given by

$$\begin{aligned}\Gamma_R(P_-, K, P_+) = & \frac{i}{2} \int \frac{d^4R}{(2\pi)^4} [C_{R2}(P_-, K, P_+, R, -R)f_R + C_\alpha(P_-, K, P_+, R, -R)r_R \\ & + C_\beta(P_-, K, P_+, R, -R)a_R].\end{aligned}\quad (92)$$

We rewrite this result by using (64). We need to compare with the expression for the polarization tensor of Fig. 20.

$$\begin{aligned}\Pi_A(P_-) = & \frac{i}{2} \int \frac{d^4R}{(2\pi)^4} [M_{R2}(P_-, -P_-, R, -R)f_R + M_C(P_-, -P_-, R, -R)r_R \\ & + M_D(P_-, -P_-, R, -R)a_R]\end{aligned}\quad (93)$$

Using  $M_N(\{P_i\}) = M_N^*(-\{P_i\})$  and  $M_{Rx}(\{P_i\}) = -M_{Rx}^*(\{P_i\})$ , with  $N = \{A, B, C, D, E, F\}$  and  $\{x, i\} = \{1, 2, 3, 4\}$  we find that (55) is satisfied.

## X. CONCLUSIONS

We have shown at finite temperature in the infrared limit that a wide class of vertex and self-energy graphs with effective vertices and corrected internal propagators satisfy a simple relation like Eq. (55). This result has two consequences. The first is that an effective expansion of ladder graphs can be realized as the iteration of a partial Schwinger–Dyson equation (Fig. 5). The second is that these ladder graphs may be combined with certain non-ladder graphs in the Schwinger–Dyson equation (Fig. 10) to give a relatively simple expression for the full self-energy (Eq. (69)). Furthermore, given an additional assumption regarding the relative contribution of the self-energy insertion to the evaluation of the full self-energy, it is seen that the ladder graphs exactly cancel against certain non-ladder graphs, leaving the one loop term of Fig. 2. This cancellation has been illustrated in some particular examples in Refs. [7,10,13]; we have shown that this feature is, for the most part, algebraic and quite general.

## XI. ACKNOWLEDGMENTS

We thank E. Petitgirard and A. Smilga for valuable discussions. This work was supported by the Natural Sciences and Engineering Research Council of Canada.

## REFERENCES

- [1] R. Pisarski, *Physica* **A158**, 146, 246 (1989); *Phys. Rev. Lett.* **63**, 1129 (1989).
- [2] V. V. Klimov, *Sov. Phys. JETP* **55**, 199 (1982).
- [3] H. A. Weldon, *Phys. Rev.* **D26**, 1384, 2789 (1982).
- [4] E. Braaten and R. D. Pisarski, *Nucl. Phys.* **B337**, 569 (1990); **B339**, 310 (1990).
- [5] J. C. Taylor and S. M. H. Wong, *Nucl. Phys.* **B346**, 115 (1990).
- [6] J. Frenkel and J. C. Taylor, *Nucl. Phys.* **B334**, 199 (1990); *Z. Phys.* **C49**, 515 (1991).
- [7] V. V. Lebedev and A. V. Smilga, *Ann. Phys. (N.Y.)* **202**, 229 (1990); *Physica* **A181**, 187 (1992).
- [8] R. D. Pisarski, *Phys. Rev.* **D47**, 5589 (1993).
- [9] F. Flechsig and A. Rebhan, *Nucl. Phys.* **B464**, 279 (1996).
- [10] U. Kraemmer, A. K. Rebhan, and H. Schulz, *Ann. Phys. (N.Y.)* **238**, 286 (1995).
- [11] A. P. de Almeida and J. Frenkel, *Phys. Rev.* **D47**, 640 (1993).
- [12] M. Carrington, *Phys. Rev.* **D45**, 2933 (1992).
- [13] M. Carrington, *Phys. Rev.* **D48**, 3836 (1993).
- [14] J. M. Cornwall and G. Tiktopoulos, *Phys. Rev.* **D15**, 2937 (1977).
- [15] J. M. Cornwall and W.-S. Hou, *Phys. Lett.* **B153**, 173 (1985).
- [16] M. Carrington, R. Kobes, and E. Petitgirard, *Phys. Rev.* **D**, in press.
- [17] L.V. Keldysh, *Zh. Eksp. Teor. Fiz.* **47**, 1515 (1964).
- [18] E.M. Lifshitz and L.P. Pitaevski, *Physical Kinetics* (Pergamon Press, Oxford, 1981).
- [19] J. Rammer and H. Smith, *Rev. Mod. Phys.* **58**, 323 (1986).
- [20] H.B. Callen and T.A. Welton, *Phys. Rev.* **83**, 34 (1951).
- [21] K.-C. Chou, Z.-B. Su, B.-L. Hao and L. Yu, *Phys. Rep.* **118**, 1 (1985).
- [22] P.A. Henning, *Phys. Rep.* **253**, 235 (1995).
- [23] T.S. Evans, *Phys. Lett* **B252**, 108 (1990); and *Nucl. Phys.* **B374**, 340 (1992).
- [24] R. Kobes, *Phys. Rev.* **D43**, 1269 (1991).
- [25] R. Fauser and P.A. Henning, private communication.
- [26] R. Kubo, *J. Phys. Soc. Japan* **12**, 570 (1957); and *Rep. Progr. Phys.* **29**, 255 (1966);  
P.C. Martin and J. Schwinger, *Phys. Rev* **115**, 1432 (1959).
- [27] M.E. Carrington and U. Heinz, *Z. für Physik C.* (in press).
- [28] M. E. Carrington, R. Kobes, and E. Petitgirard, hep-ph/9708412.

# FIGURES

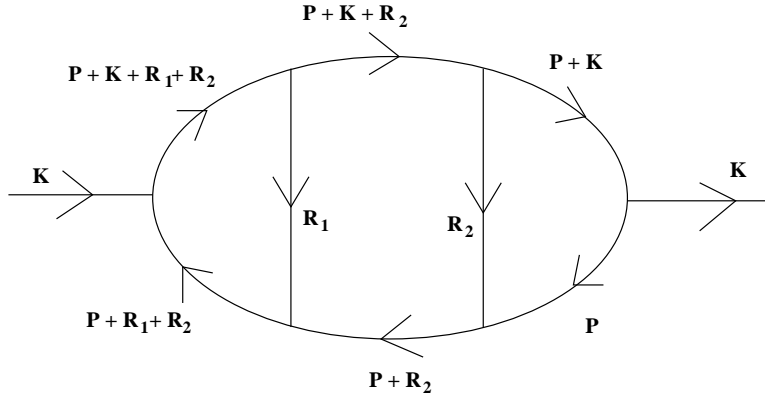


FIG. 1. A three-loop self-energy ladder graph

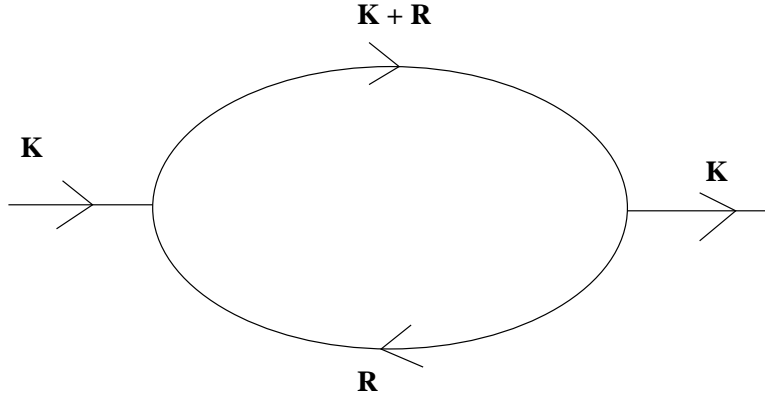


FIG. 2. A one-loop self-energy graph

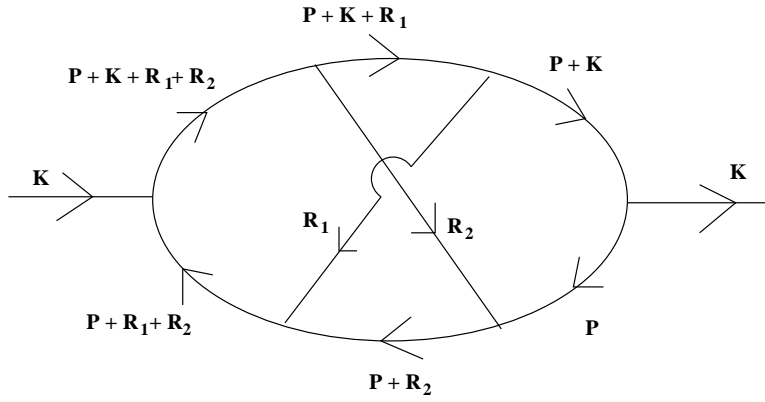


FIG. 3. A three-loop self-energy non-ladder graph

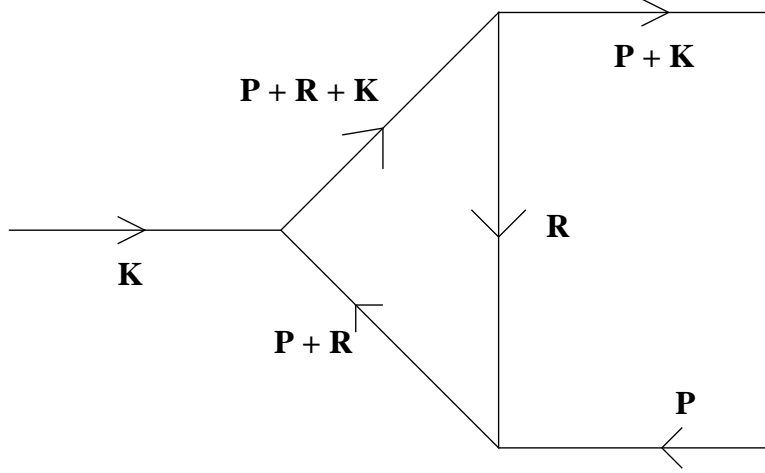


FIG. 4. A one-loop vertex graph

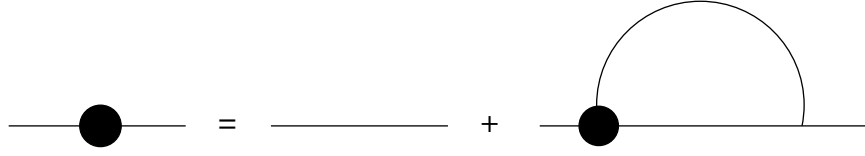


FIG. 5. A partial Schwinger–Dyson equation for the full self-energy which generates the ladder graph resummation

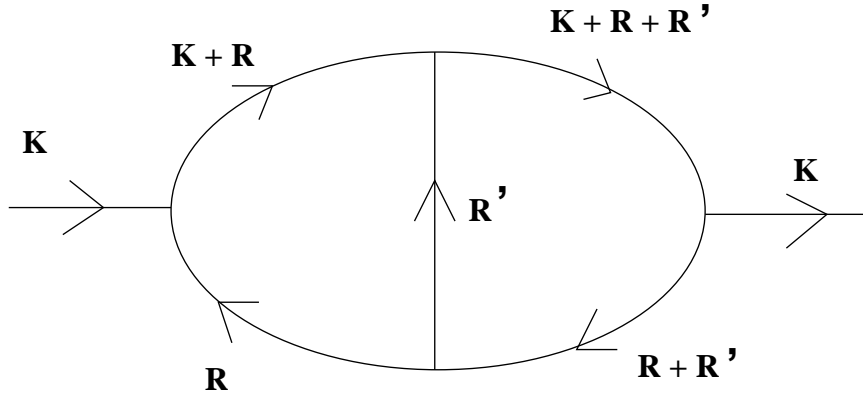


FIG. 6. A two-loop ladder graph contribution to the self-energy

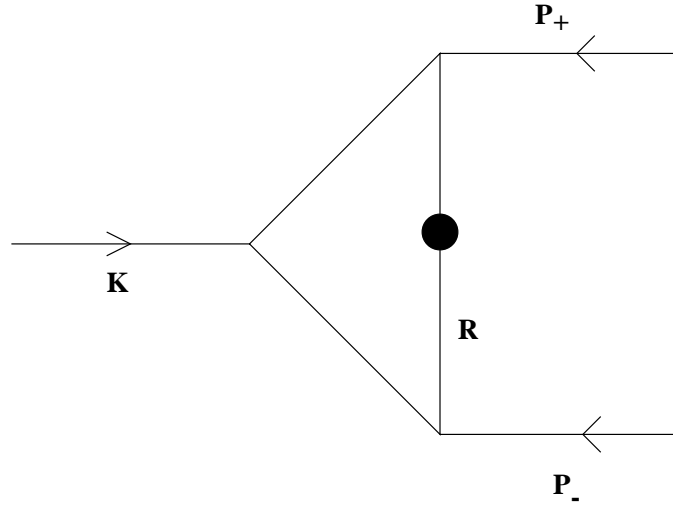


FIG. 7. Three point vertex with corrected internal line

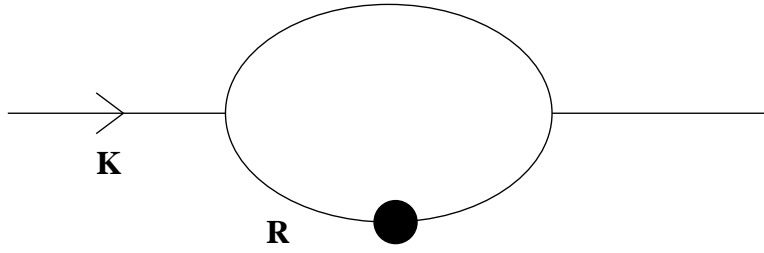


FIG. 8. Polarization tensor associated with Fig. 7

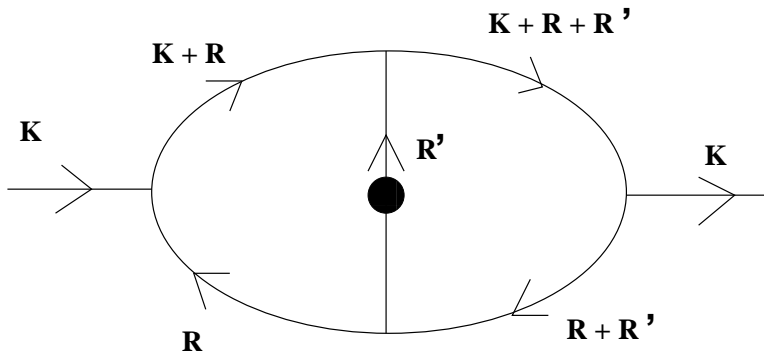


FIG. 9. Ladder graph corresponding to Fig. 7 with a corrected internal line

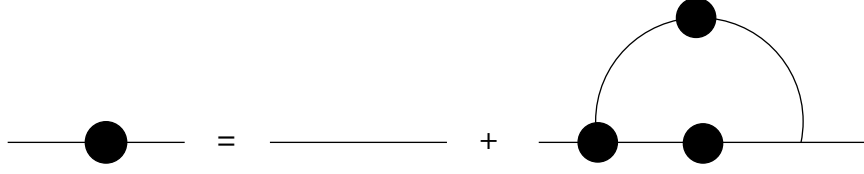


FIG. 10. The Schwinger–Dyson equation for the full self-energy

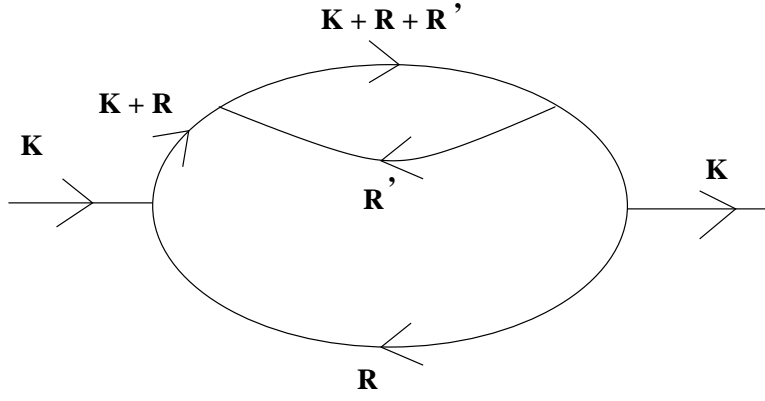


FIG. 11. Two-loop graph with a self-energy correction

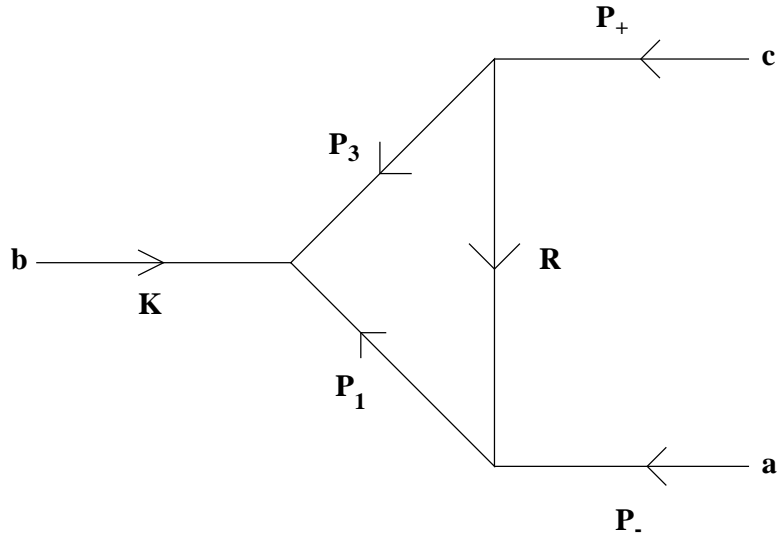


FIG. 12. Three point vertex



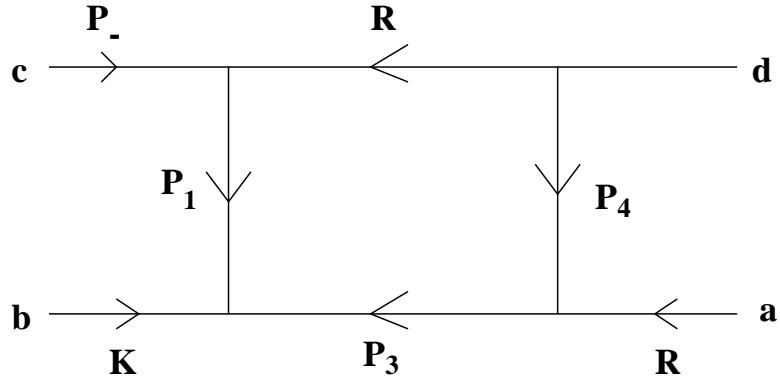


FIG. 13. Four point vertex

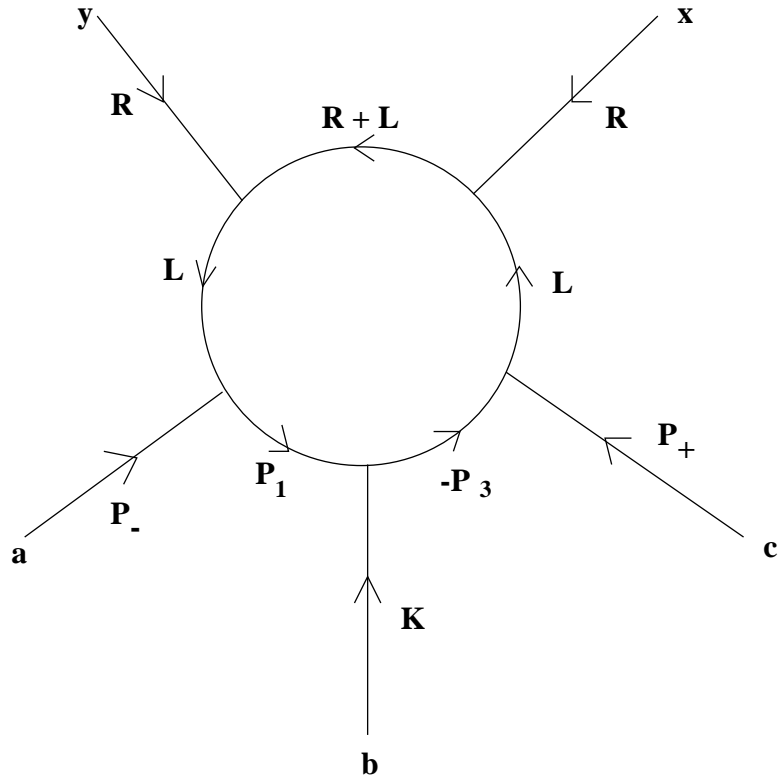


FIG. 14. Five point vertex graph

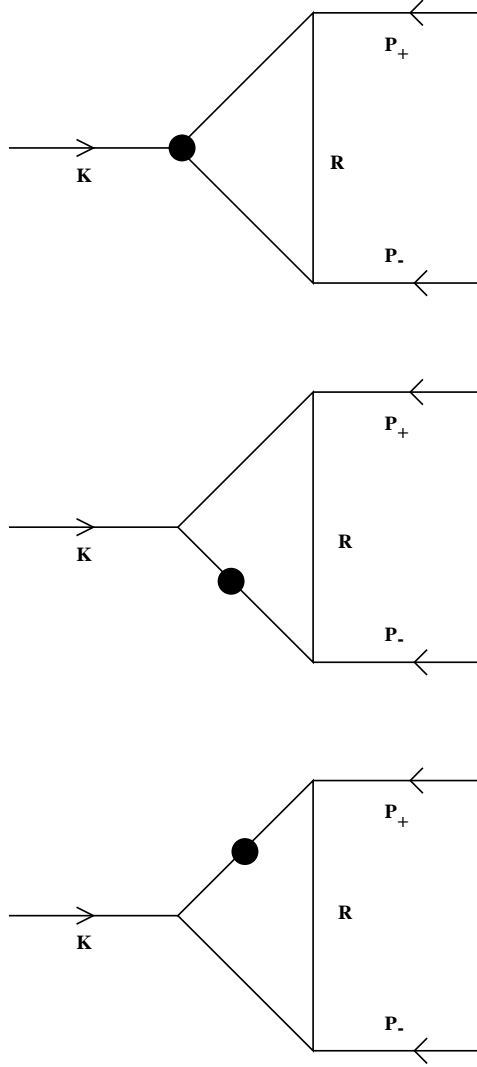


FIG. 15. Three point vertex with corrected internal line and vertices

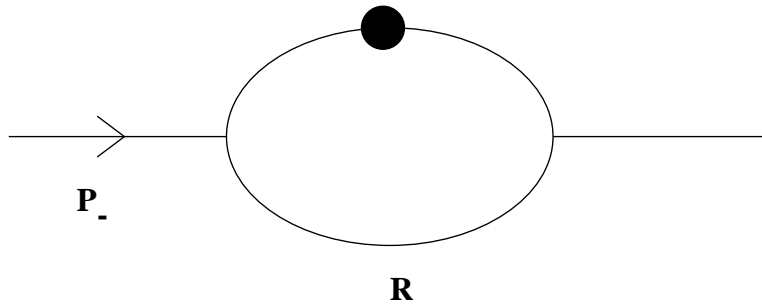


FIG. 16. Polarization tensor associated with Fig. 15

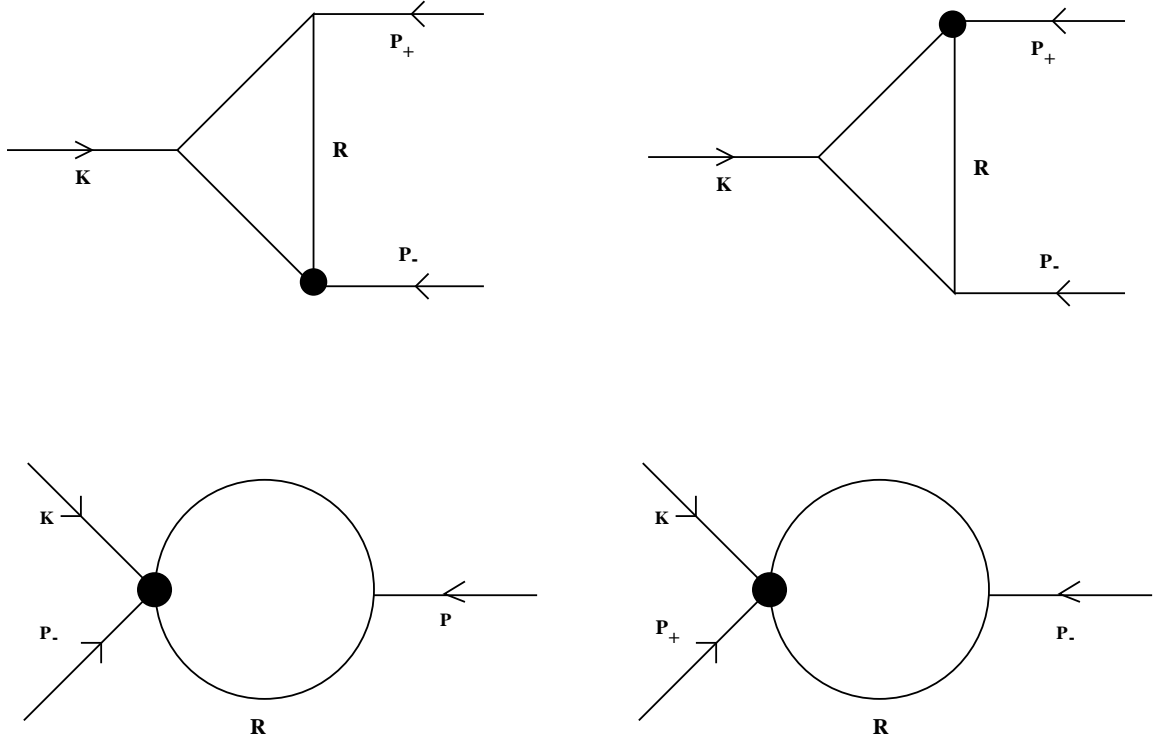


FIG. 17. Three point vertices with corrected internal vertices

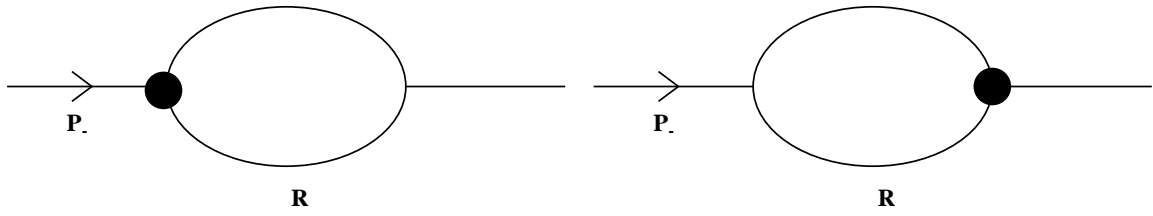


FIG. 18. Polarization tensor associated with Fig. 17

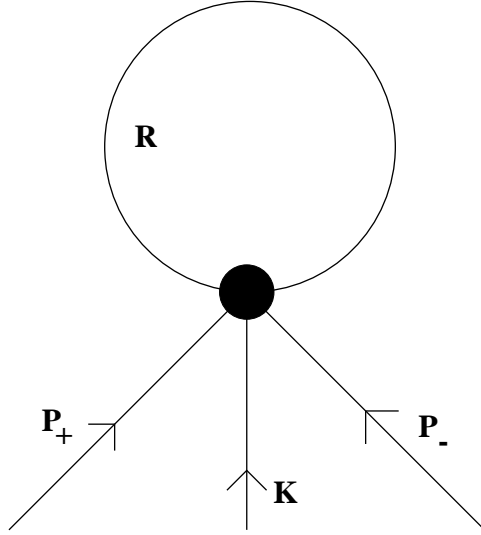


FIG. 19. Five point vertex

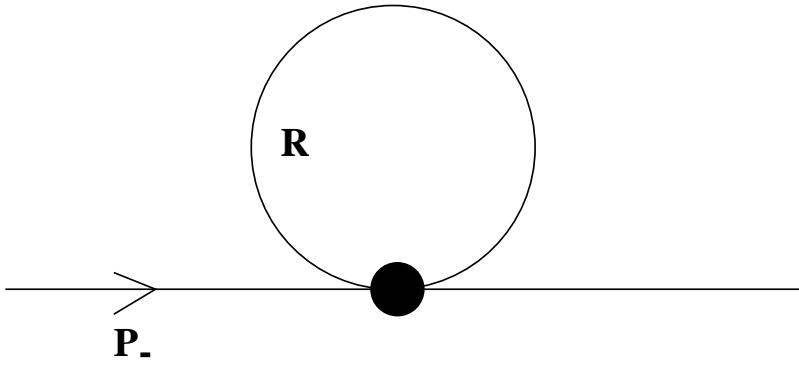


FIG. 20. Polarization tensor associated with Fig. 19